



HAL
open science

Optimized Cas9 expression systems for highly efficient Arabidopsis genome editing facilitate isolation of complex alleles in a single generation

Jana Ordon, Mauro Bressan, Carola Kretschmer, Luca Dall'osto, Sylvestre Marillonnet, Roberto Bassi, Johannes Stuttmann

► To cite this version:

Jana Ordon, Mauro Bressan, Carola Kretschmer, Luca Dall'osto, Sylvestre Marillonnet, et al.. Optimized Cas9 expression systems for highly efficient Arabidopsis genome editing facilitate isolation of complex alleles in a single generation. *Functional and Integrative Genomics*, 2019, 20 (1), pp.151-162. <10.1007/s10142-019-00665-4>. <hal-04850160>

HAL Id: hal-04850160

<https://hal.science/hal-04850160v1>

Submitted on 19 Dec 2024

HAL is a multi-disciplinary open access archive for the deposit and dissemination of scientific research documents, whether they are published or not. The documents may come from teaching and research institutions in France or abroad, or from public or private research centers.

L'archive ouverte pluridisciplinaire HAL, est destinée au dépôt et à la diffusion de documents scientifiques de niveau recherche, publiés ou non, émanant des établissements d'enseignement et de recherche français ou étrangers, des laboratoires publics ou privés.



Distributed under a Creative Commons CC BY-NC-ND 4.0 - Attribution - Non-commercial use - No Derivative Works - International License

Title: Optimized Cas9 expression systems for highly efficient Arabidopsis genome editing facilitate isolation of complex alleles in a single generation

Jana Ordon¹, Mauro Bressan², Carola Kretschmer¹, Luca Dall'Osto², Sylvestre Marillonnet³, Roberto Bassi², Johannes Stuttmann^{1*}

1 – Institute for Biology, Department of Plant Genetics, Martin Luther University Halle-Wittenberg, Weinbergweg 10, 06120 Halle (Saale), Germany

2 - Dipartimento di Biotecnologie, Università di Verona, Strada Le Grazie 15, 37134 Verona, Italy

3 - Department of Cell and Metabolic Biology, Leibniz Institute of Plant Biochemistry, Weinberg 3, 06120 Halle (Saale), Germany

* Corresponding author: Johannes Stuttmann, Martin Luther University of Halle (Saale), Weinbergweg 10, 06120 Halle, Germany, phone +49-345-5526345, fax +49-345- 5527151, [email](#), ORCID ID orcid.org/0000-0002-6207-094X

Jana Ordon	jana.ordon@gmx.de
Mauro Bressan	mauro.bressan@univr.it
Carola Kretschmer	carola.kretschmer@genetik.uni-halle.de
Sylvestre Marillonnet	smarillo@ipb-halle.de
Luca Dall'Osto	luca.dallosto@univr.it
Roberto Bassi	roberto.bassi@univr.it
Johannes Stuttmann	johannes.stuttmann@genetik.uni-halle.de

Running title: Genome Editing Efficiency in Arabidopsis

Key Words: *SpCas9*; Arabidopsis; Promoter; FAST marker; Lhcb1; RPS5a

Acknowledgements

We acknowledge Bianca Rosinsky for taking care of plant growth facilities and growing plants. Ulla Bonas is acknowledged for generous support. This work was funded by GRC grant STU 642-1/1 (Deutsche Forschungsgemeinschaft, DFG) and seed funding by the CRC 648 (DFG) to Johannes Stuttmann. Mauro Bressan and Luca Dall'Osto were supported by University of Verona (Program CooperInt2017 and HuntingLight Ricerca di Base 2015).

1 **Abstract**

2 Genetic resources for the model plant *Arabidopsis* comprise mutant lines defective in almost any single gene
3 in reference accession Columbia. However, gene redundancy and/or close linkage often render it extremely
4 laborious or even impossible to isolate a desired line lacking a specific function or set of genes from
5 segregating populations. Therefore, we here evaluated strategies and efficiencies for the inactivation of
6 multiple genes by Cas9-based nucleases and multiplexing. In first attempts, we succeeded in isolating a
7 mutant line carrying a 70 kb deletion, which occurred at a frequency of ~1.6% in the T₂ generation, through
8 PCR-based screening of numerous individuals. However, we failed to isolate a line lacking *Lhcb1* genes,
9 which are present in five copies organized at two loci in the *Arabidopsis* genome. To improve efficiency of
10 our Cas9-based nuclease system, regulatory sequences controlling Cas9 expression levels and timing were
11 systematically compared. Indeed, use of *DD45* and *RPS5a* promoters improved efficiency of our genome
12 editing system by approximately 25-30-fold in comparison to the previous ubiquitin promoter. Using an
13 optimized genome editing system with *RPS5a* promoter-driven Cas9, putatively quintuple mutant lines
14 lacking detectable amounts of Lhcb1 protein represented approximately 30% of T₁ transformants. These
15 results show how improved genome editing systems facilitate the isolation of complex mutant alleles,
16 previously considered impossible to generate, at high frequency even in a single (T₁) generation.

17

18 **Introduction**

19 Sequence-specific nucleases (SSNs) based on *SpCas9*, which derives from the *Streptococcus pyogenes*
20 CRISPR/Cas system, are currently the most commonly used tool for genome editing in plants and animals
21 (reviewed in Cesar et al., 2016). *SpCas9* (hereafter termed Cas9) and related RNA-guided nucleases (RGNs)
22 are directed to DNA target sequences by a guide RNA incorporating into the nuclease protein. The guide RNA
23 may consist of a chimera from base-pairing between a CRISPR RNA (crRNA) and a trans-activating RNA
24 (tracrRNA), or crRNA and tracrRNA may be collapsed into a single guide RNA (sgRNA; Jinek et al., 2012). In
25 either case, the variable stretch of crRNA/sgRNA base-pairs with complementary target DNA sequences
26 flanked by a protospacer-adjacent motif (PAM, NGG for unmodified Cas9). Cas9 functions in its native
27 configuration as a nuclease and cleaves target sequences, but can be considered as a programmable DNA-
28 binding scaffold for tethering diverse activities or functionalities to precise chromatin positions. As such, e.g.
29 transcriptional regulators, chromatin modifiers or base editors were constructed on the basis of catalytically
30 inactive Cas9 (*dCas9*), or fluorescent protein fusions were exploited for live cell imaging (Chavez et al., 2016;
31 Chen et al., 2016; Dominguez et al., 2016; Komor et al., 2016; Ren et al., 2018).

32 In the nuclease mode, Cas9 generates either blunt-ended double-strand breaks (preferentially three base
33 pairs upstream of the PAM sequence), or single-strand breaks when converted to a nickase (Jinek et al.,
34 2012; Ran et al., 2013). Gene targeting may be achieved from both types of lesions, but remains technically
35 challenging, at least in plants (Fauser et al., 2014; Shi et al., 2017). In contrast, the disruption of genes
36 through error-prone repair of double strand breaks by non-homologous end-joining (NHEJ) is now routinely
37 used for reverse genetics approaches in many different plant systems (reviewed in Malzahn et al., 2017).
38 When using RGNs for precision gene editing in crop improvement, the specificity of the enzyme may be of
39 major importance. Indeed, delivery of ribonucleoprotein complexes has been reported to minimize RGN off-
40 target activity, and is also preferable to avoid regulation of the final product (Woo et al., 2015; Huang et al.,
41 2016; Wolt et al., 2016; Zhang et al., 2016; Liang et al., 2017). In contrast, *Agrobacterium*-facilitated
42 transformation and *in planta* expression yet remains the most important approach for RGN delivery in basic
43 research. Efficiency in this case mainly depends on timing and levels of expression of nuclease and sgRNA
44 and efficient nuclear import. Although high expression levels may increase off-target activity, these effects
45 can be mitigated, e.g., through analysis of multiple alleles, and efficiency is generally at prime. In some
46 species, as e.g. rice, high efficiencies for genome editing regularly approaching 100% in T₀ plants (with Cas9
47 or Cpf1) were reported, suggesting that further optimization is not required in this respect (Mikami et al.,
48 2015; Tang et al., 2017). However, especially in Arabidopsis, the genetic analyses workhorse, genome editing
49 efficiencies are often comparably low, and severely vary between different studies. In the Arabidopsis
50 system, transformation does not depend on somatic embryogenesis, as T-DNAs are directly delivered to
51 female ovules during floral dip transformation (Ye et al., 1999; Desfeux et al., 2000). Accordingly, T-DNA-
52 encoded SSNs are subsequently expressed (or not) in different cell types of the developing embryo, and
53 expression levels and timing will be decisive for efficiency and germ line entry of genome modifications.
54 Indeed, exceptionally high genome editing efficiencies were reported when *RPS5a* or *DD45* promoters (or
55 derivatives) were used for Cas9 expression (Wang et al., 2015; Mao et al., 2016; Tsutsui and Higashiyama,
56 2017). These effects were mainly attributed to activity of these promoters in early embryogenesis. However,
57 the cross-study comparison of genome editing efficiencies is of limited validity, as differences between
58 constructs go beyond the use of a particular promoter. Especially the sgRNA/target site represents a major
59 variable affecting genome editing efficiency, and also further differences between vectors may have
60 profound and unexpected consequences.

61 Here, we systematically compared regulatory elements in order to determine improved Cas9 expression
62 systems for Arabidopsis genome editing. While a previously used *ubiquitin* promoter-driven Cas9 produced
63 mutants in the T₂ generation and at moderate frequencies only, optimized expression systems were highly
64 efficient in the T₁ generation. Indeed, this enabled us to isolate a putative quintuple mutant lacking
65 detectable amounts of Lhcb1 protein in a single generation and at high frequencies, while we had failed to

66 isolate this mutant line prior to system optimization. This shall guide further optimization of Arabidopsis
67 genome editing systems, and also researchers in their future choice of system.

68

69 **Material and Methods**

70 **Plant material and transformation**

71 Arabidopsis accession Landsberg *erecta* (*Ler*), the *old3-1* mutant line (Tahir et al., 2013), accession Columbia
72 and the NoMxB3 quadruple mutant line were used. The NoM line is published (Dall'Osto et al., 2017), and a
73 T-DNA insertion in At5g54270 (*Lhcb3*; NASC N520342) was introgressed to generate the NoMxB3 quadruple
74 mutant. Plants were grown in soil at a 19°C: 22°C night: day cycle (200 $\mu\text{E}/\text{m}^2\cdot\text{s}$, 60% relative humidity)
75 under short (16h dark, 8h light) or long (8h dark, 16h light) day conditions. To suppress autoimmunity, plants
76 were grown at a 26°C: 28°C night: day cycle in a growth cabinet (200 $\mu\text{E}/\text{m}^2\cdot\text{s}$, 60% relative humidity) with
77 either short day or long day conditions. Plants were transformed by floral dip as described (Logemann et al.,
78 2006), and *old3-1* plants were cultivated at 28°C to suppress autoimmunity for transformation.

79

80 **Molecular cloning**

81 Golden Gate technology (Engler et al., 2008) was used for all cloning tasks, and the Modular Cloning and
82 Plant Parts toolkits were used (pICH/pAGM/pICSL vectors; Engler et al., 2014). Generally, 20 fmol of DNA
83 modules were used for Golden Gate reactions with either *Bsa*I, *Bsm*BI or *Bpi*I and T4 DNA Ligase. Reactions
84 were carried out in a PCR cycler (2 min 37°C, 5 min 16°C, 10-55 cycles; terminated by 10 min 50°C and 10 min
85 80°C steps), and transformed either into *E. coli* TopTen or *ccdB* survival II cells (Invitrogen; distributed by
86 Thermo Fisher). To generate the adaptable nuclease activity reporter (pJOG367), a linker sequence was
87 appended to a *ccdB* cassette (lacking *Bsm*BI and *Bsa*I sites) by PCR amplification, and subcloned in a custom
88 cloning vector (pJOG397) to yield pJOG395. Similarly, an amplicon of a *GUS* gene with introns (Engler et al.,
89 2014) and a linker sequence was subcloned to yield pJOG396. These modules were subsequently assembled
90 together with a 35S promoter (pICH51277) and an *ocs* terminator (pICH41432) in a Level 1 recipient
91 (pICH47732) to yield pJOG367. Target sequences are inserted in this adaptable reporter scaffold as
92 hybridized oligonucleotides by a *Bsm*BI Golden Gate reaction (Online Resource 1). Promoter fragments were
93 amplified by PCR, internal *Bsa*I and *Bpi*I restriction sites domesticated and subcloned into pICH41295. The
94 previously reported *rbcS E9* terminator fragment (Wang et al., 2015) was amplified from *Pisum sativum*
95 genomic DNA and subcloned into pICH41276. All genome editing constructs were assembled as previously
96 described (Ordon et al., 2017) and essentially following the Modular Cloning strategy (Weber et al., 2011). A

97 previously published *hCas9* coding sequence (Belhaj et al., 2013) was used for assemblies, and sgRNAs were
98 driven by a 90 nt promoter fragment of *Arabidopsis* U6-26, as previously described (Ordon et al., 2017).
99 Further details and oligonucleotide sequences are available upon request. Genbank files for most important
100 modules and nuclease vectors are provided in Online Resource 2.

101

102 **sgRNA selection and deletion screening**

103 A local instance of CasOT (Xiao et al., 2014) was used to identify specific sgRNAs for generation of the
104 $\Delta dm2a-g$ mutant. Sequence windows flanking the *DM2a* and *DM2g* genes, respectively, were defined for
105 selection of targets, and a PacBio assembly of the Landsberg *erecta* genome was used as reference
106 (<https://www.pacb.com>). Specific sgRNAs were subsequently evaluated with the sgRNA designer tool
107 (Doench et al., 2014; Doench et al., 2016) to select those with highest predicted activity. For editing of the
108 *DM2h* gene (promoter comparison), the target sites TGATTTCTGCTAATTCATCAAGG and
109 TTATTGATAATAATATAGAGAGG were selected. ChopChop (Labun et al., 2016) was used for selection of
110 target sites within *Lhcb1* genes, and potential sites were further manually curated and selected. The
111 following target sites were used for sgRNA design: CGCGGCAGTTCGGTCCGCCAAGG [1],
112 GCCGACCTGCCGCCTAATTGTGG [2], CACTGCAGAGATATTGAACGAGG [3], GTTATATAATGCTTGATGGATGG [4]
113 for the $\Delta dm2a-g$ deletion, and GGTTACAGATCTTCAGCGACGG [1], ATGGACCCAAGTACTTGACTCGG [2],
114 TGTGGATAACTTCTAGCTCACGG [3], GGCTACTCAAGTTATCCTCATGG [4], GAAGCGCCGTGTGACAATGAGG [5],
115 AGAAGTTATCCACAGCAGGTGGG [6], GAGGACTTGCTTTACCCCGGTGG [7], AGGGGAGGAGAGACCATTGTGG
116 [8] for *Lhcb1* genes. Oligonucleotides JS1382/83 (TGCAGCTGAAGATCATGGC/GACTAGCGATTGTGTCCATC)
117 were used for detection of a $\Delta dm2a-g$ deletion allele. Oligonucleotides MB1/MB4 ("PCR *Lhcb1.1/.2/.3*";
118 AAAGCCTCTGGGTCCGTAGCA/TCTGGGTCCGTAGCCAAACCC) and MB6/MB7 ("PCR *Lhcb1.4/.5*";
119 CCGGCGACTCTGTAGCCCTCA/TCCGGCGACTCTGTAGCCTTC) were used to screen for deletions at *Lhcb1* loci.

120

121 **Transgenic plant selection and estimation of genome editing efficiencies**

122 For seed fluorescence-based selection using the FAST marker (Shimada et al., 2010), T₁ or T₂ seeds were
123 spread on moist Whatman paper, and observed under a motorized SteREO Discovery.V12 microscope (Zeiss)
124 connected to an AxioCam MRc camera. Pictures were taken under bright field conditions or UV illumination
125 and using an RFP filter set. For selection of transgenic plants from *old3-1* transformations, seedlings were
126 grown at 28°C, treated 3 – 4 times with BASTA and resistant plants transferred to new soil. For promoter
127 comparison, T₁ seedlings were transferred to 22°C, onset of autoimmunity was scored after 8d, and

128 transgenic plants transferred back to 28°C to obtain T₂ seeds. T₂ seeds were directly grown at 22°C in short
129 day conditions, and phenotypes scored 20 dag to calculate editing frequencies in individual T₂ families.
130 Plants were transformed with a construct conferring Hygromycin resistance (pDGE277) for generation of an
131 *lhcb1* mutant line. Seeds were surface-sterilized, grown on MS 1/10 plates containing 0,5% sucrose,
132 Hygromycin B (25 µg/ml) and Carbenicillin (100 µg/ml), and Hygromycin-resistant seedlings selected 15 dag.

133

134 **Gel electrophoresis, immunoblotting and sample preparation**

135 SDS-PAGE analysis was performed with the Tris-Tricine buffer system (Schagger and von Jagow, 1987). For
136 immunodetection, samples corresponding to 0.5 µg of Chlorophyll were loaded for each sample and
137 electroblotted on nitrocellulose membranes. Proteins were detected with alkaline phosphatase-conjugated
138 secondary antibodies purchased from Sigma-Aldrich (A3687). Primary antibodies used were α-Lhcb1 (AS01
139 004), α-PsaA (AS06 172), α-PsbB/CP47 (AS04 038) from Agrisera.

140

141 **Transient genome editing efficiency assays**

142 For GUS-based nuclease assays, an sgRNA directed against the target site TATATAAACCCCTCCAACCAGG
143 was used. This target site was inserted into the adaptable reporter plasmid (pJOG367). *Agrobacterium*
144 strains containing reporter or nuclease-encoding constructs were infiltrated alone or in a 1:1 ratio at an
145 OD₆₀₀ = 0.6 into leaves of four different *N. benthamiana* plants. Tissue samples of individual plants were
146 treated as replicates, and GUS activity was determined as previously described (Ordon et al., 2017). GUS
147 activity was normalized to the reporter alone, which was arbitrarily set to 1.

148

149 **Results**

150 **Generation of complex alleles with *ubiquitin* promoter-driven Cas9 in Arabidopsis**

151 We had previously developed a Golden Gate cloning-based toolkit for highly multiplexed genome editing in
152 dicotyledonous plants (Ordon et al., 2017). In this system, expression of sgRNAs is driven by the Arabidopsis
153 U6-26 promoter, and several different promoters were provided for Cas9 expression. Using *ubiquitin*
154 promoter-driven Cas9 (*pPcUbi4-2*, from parsley), a 120 kb deletion encompassing the *DM2* cluster of
155 *Resistance* genes in accession Landsberg *erecta* (*Ler*) was previously generated (Ordon et al., 2017). The
156 respective *Δdm2* deletion allele could be phenotypically selected, and occurred at low frequencies only (~

157 0.5%) among T₂ individuals. To evaluate strategies for and feasibility of generating large deletion alleles not
158 linked to a phenotype, we attempted deletion of ~ 70 kb within the DM2^{Ler} cluster containing all genes of the
159 cluster except DM2h (Fig. 1a). The DM2^{Ler} cluster encodes 7-8 complete or truncated *Resistance* genes
160 (DM2a-h, or RPP1-like^{Ler} R1-R8) most similar to RPP1, conferring resistance to the obligate biotrophic
161 oomycete *Hyaloperonospora arabidopsidis* in accession Wassilijewska (Botella et al., 1998; Alcazar et al.,
162 2009; Chae et al., 2014). The function(s) of the DM2^{Ler} locus remain yet unknown, but one or several DM2^{Ler}
163 genes provoke constitutive activation of immune responses (autoimmunity) when combined in a single
164 genetic background with different “inducers”: Alleles of *STRUBBELIG-RECEPTOR FAMILY 3* originating from
165 the South Asian accessions Kashmir and Kondara (SRF3^{Kas/Kond}; Alcazar et al., 2010), a transgene encoding for
166 ENHANCED DISEASE SUSCEPTIBILITY1 fused to YFP and an SV40 nuclear localization signal (EDS1-YFP^{NLS};
167 Stuttmann et al., 2016) or the *onset of leaf death3-1* allele affecting a cytosolic O-acetylserine(thiol)lyase
168 (*old3-1*; Tahir et al., 2013). The DM2h gene is required for all cases of autoimmunity, but the contribution of
169 additional DM2 genes remains unknown (Alcazar et al., 2014; Stuttmann et al., 2016). The $\Delta dm2a-g$ deletion
170 was conducted in the *Ler old3-1* background, and plants were grown at 28°C to suppress temperature-
171 sensitive autoimmunity and seedling necrosis in this line (Tahir et al., 2013).

172 For deletion of DM2a-g, a construct containing Cas9 driven by the pPcUbi4-2 promoter and four sgRNAs
173 directed against sites flanking the targeted region was transformed into *Ler old3-1* plants (Fig. 1a). T₁ plants
174 were selected by BASTA resistance, and T₂ populations consisting of 4-5 T₁ plants assembled. 96 DNA pools
175 containing 7-11 T₂ plants each (equivalent of ~ 850 T₂ plants) were screened by PCR with oligonucleotides
176 flanking the targeted region for occurrence of a $\Delta dm2a-g$ deletion allele (Figs. 1a,b). A clear signal of the
177 expected size was detected in 14/96 DNA pools, representing 15% of pools or approximately 1.6% of T₂
178 plants considering a single line with a deletion allele in each PCR-positive pool. Selected pools were
179 deconvoluted, and single plants screened (Fig. 1c). For some pools, only a weak signal corresponding to the
180 deletion allele was detected among single plants (pool #8 in Fig. 1c), but most pools contained 1-2 plants
181 positive for the deletion allele (pool #89 in Fig. 1c). T₃ seeds were obtained for these single plants, and PCR-
182 screened for segregation of the $\Delta dm2a-g$ allele and Cas9. From analysis of 96 T₃ plants, several lines
183 homozygous for the $\Delta dm2a-g$ allele (absence of DM2c, boxed lanes in Fig. 1d) could be isolated, but all still
184 contained the genome editing transgene, as detected by presence of Cas9. Outcrossing of the Cas9 construct
185 is most likely not required for most experimental settings. However, sequencing of the $\Delta dm2a-g$ deletion
186 allele in one of the isolated homozygous lines revealed that it still contained an intact sgRNA target site (Fig.
187 1e), suggesting it might not be fully stable in subsequent generations. Summarizing, PCR-based isolation of
188 large deletion alleles is feasible with the used genome editing system (containing pPcUbi-driven Cas9), but
189 deletions occur at low frequency, and isolation requires extensive screening.

190 Furthermore, we attempted to generate a mutant lacking Lhcb1 (chlorophyll a/b binding protein 1, CAB), a
191 major subunit of light-harvesting complex II (LHCII) and the most abundant membrane protein in nature
192 (Galka et al., 2012; Su et al., 2017). The *Arabidopsis thaliana* genome contains five *Lhcb1* genes, which are
193 organized in tight linkage groups on chromosomes 1 and 2 (Fig. 1f). For inactivation of *Lhcb1* genes, a
194 genome editing construct (with pPcUbi4-2-driven Cas9) containing eight sgRNAs was constructed, and
195 transformed into Columbia (Col) wild type plants. *Lhcb1* genes in each linkage group share high sequence
196 homology, and sgRNAs were designed to target four sites with perfect match in each *Lhcb1* gene (Fig. 1f).
197 Thus, genome editing activity might produce SNPs within individual genes, or larger deletions between
198 target sites. As for *Δdm2a-g*, T₂ plants were PCR-screened for occurrence of larger deletions with flanking
199 oligonucleotides. From screening ~ 200 T₂ plants, no line PCR-positive for a deletion in either of the linkage
200 groups could be detected. Also, none of ~ 400 plants visually inspected showed the pale green phenotype
201 expected for lines with reduced Lhcb1 levels (Pietrzykowska et al., 2014). We concluded that efficiency of
202 our genome editing system was not sufficient for convenient isolation of complex or highly multiplexed
203 alleles.

204

205 **Improved genome editing efficiencies through optimized Cas9 expression systems**

206 To improve efficiency of our genome editing system, we focused on regulatory elements controlling Cas9
207 expression. The *rbcS E9* terminator from pea (*Pisum sativum*) was previously described to positively affect
208 genome editing efficiencies in comparison to the *nos* terminator (*nopaline synthase; Agrobacterium*
209 *tumefaciens*) in several independent constructs and transformations (Wang et al., 2015), suggesting
210 stabilization of the respective mRNA. To more generally test the importance of transcriptional terminators
211 for Cas9 activity, we wanted to compare genome editing efficiencies of nuclease constructs differing only in
212 3'UTR sequences and transcriptional terminators for Cas9 expression. Since mRNA stabilization should not
213 be strictly limited to a particular plant system, genome editing efficiencies were compared in quantitative,
214 transient assays in *Nicotiana benthamiana* (*N. benth.*). For this, an adaptable genome editing efficiency
215 reporter was first constructed (Online Resource 1). This adaptable reporter allows insertion of user-defined
216 target sequences in a linker region of a β -glucuronidase (*uidA*) gene. Insertion of a target sequence disrupts
217 the *GUS* reading frame, which can be restored by RGN-mediated cleavage and repair through the NHEJ
218 pathway (Online Resource 1). Transient co-expression of reporter constructs and corresponding nucleases in
219 *N. benth.* faithfully restored GUS activity, and reporter/nuclease combinations showed variable GUS
220 activities potentially reflecting sgRNA efficacy (Online Resource 1). Nine minimalistic nuclease constructs
221 containing only the sgRNA transcriptional unit and 35S promoter-driven Cas9 with different transcriptional
222 terminators were quantitatively compared for genome editing efficiency (Fig. 2a). Across multiple biological

223 replicates, no significant and reproducible differences were measured (Fig. 2b). However, high genome
224 editing efficiencies were obtained in all replicates when using the *rbcS E9* terminator. This corroborates the
225 previous notion that the *rbcS E9* terminator is well-suited for Cas9 expression even when combined with
226 *hCas9* (human codon-optimized), in contrast to previously used *zCas9* (*Zea mays* codon-optimized; Wang et
227 al., 2015). Furthermore, this is in line with potential masking of the beneficial effects of this terminator by
228 expression of Cas9 by strong constitutive promoters (Wang et al., 2015). Since no other terminator out-
229 competed *rbcS E9*, this was used for further experiments.

230 Next, different promoters were tested for their effect on genome editing efficiency. As far as we are aware,
231 the 35S promoter (e.g. Feng et al., 2013; Ordon et al., 2017), several different *ubiquitin* promoters (e.g. Mao
232 et al., 2013; Fauser et al., 2014; Peterson et al., 2016), egg cell-specific promoters or derivatives (*DD45* and
233 *EC1.2-EC1.1*; Wang et al., 2015; Mao et al., 2016), promoters of *APETALA1* (*AP1*; Gao et al., 2015),
234 *INCURVATA2* (*ICU2*; Hyun et al., 2015), *YAO* (Yan et al., 2015), *SPOROCTELESS* and *LAT52* (Mao et al., 2016),
235 *MGE1/2/3* (Eid et al., 2016), *HISTONE H4* and *EF1 α* (Osakabe et al., 2016) and *RIBOSOMAL PROTEIN S5a* and
236 *WUSCHEL RELATED HOMEBOX 2* (*RPS5a* and *WOX2*; Tsutsui and Higashiyama, 2017) were previously used
237 to drive Cas9 expression for Arabidopsis genome editing. The occurrence of homozygous mutants in the T₁
238 generation at high frequencies was mainly reported for the *RPS5a* promoter and the egg cell-specific *DD45*
239 promoter or derivatives (Wang et al., 2015; Mao et al., 2016; Tsutsui and Higashiyama, 2017), and also for
240 the meiosis-specific *MGE1* promoter (Eid et al., 2016). We decided to focus on the *RPS5a* and *DD45*
241 regulatory elements, and to compare these with several popular promoters not reported to generate
242 mutations in T₁ generation (p35S, pPcUbi, p*AP1*, p*ICU2*) and two further promoters not previously employed
243 for genome editing (p*GILT*, p*ALB*; see Online Resource 2 for sequence details for used promoter fragments).

244 Promoter fragments were used for driving Cas9 expression (terminated by *trbcS E9*) in genome editing
245 vectors containing two sgRNA transcriptional units, a BASTA resistance cassette and also the FAST marker for
246 seed coat fluorescence-based identification of transgenic plants (Fig. 3a; Shimada et al., 2010). The
247 positioning and orientation of the FAST cassette was altered in comparison to vectors we had previously
248 generated and containing this element (Ordon et al., 2017). Although transgenic plants could be selected by
249 monitoring seed fluorescence with the previous vector architecture, the antibiotic/herbicide resistance
250 markers neighboring the FAST cassette were not functional, and no genome editing activity was observed in
251 several independent experiments and with different sgRNAs in Arabidopsis. This shall act as a cautionary
252 note for use of the FAST marker in novel assemblies, and exemplifies the synthetic biology crux that a
253 system's performance is not simply the sum of its components. With the novel vector architecture,
254 transgenic plants could conveniently be selected by herbicide resistance in the T₁ generation (Fig. 3b), and
255 also the FAST marker was functional for selection/counter-selection in T₁ and T₂ generations (Fig. 3c). The

256 eight constructs differing only in promoter fragments driving Cas9 expression contained sgRNAs for targeting
257 of the *DM2h* gene of the *DM2^{Ler}* cluster, and were transformed into *Ler old3-1* plants (cultivated at 28°C to
258 suppress autoimmunity). Inactivation of *DM2h* rescues the autoimmune phenotype of the *old3-1* line in a
259 dose-dependent manner, and both heterozygous (*DM2h/dm2h*) and homozygous (*dm2h/dm2h*) plants can
260 be phenotypically identified by simple survival at different temperature regimes (Ordon et al., 2017).

261 Genome editing in the T₁ generation was first tested by shifting BASTA-resistant transformants from 28°C to
262 22°C. At this temperature, inactivation of a single *DM2h* allele is sufficient to suppress autoimmunity of the
263 parental line. Eight days after shifting, all plants showed signs of autoimmunity, arguing against efficient
264 genome editing with any of the constructs/promoters in this generation and with the used sgRNAs. Five to
265 eleven BASTA-resistant T₁ plants of each transformation were further cultivated at 28°C to obtain T₂ seeds.
266 T₂ plants were grown alongside control plants (*Ler*, *Ler old3-1*) at 22°C, and *old3-1* plants became necrotic
267 after 20 d of growth (Fig. 3d). Although only limited numbers of T₂ pools were analyzed for constructs
268 containing different promoters, obvious differences for the frequencies of phenotypically rescued (*Ler*-like),
269 and thus genome-edited, plants became evident: Rescued plants were not present upon expression of Cas9
270 by 35S, *ALB* or *GILT* promoters, were rare for *ICU2*, *AP1* and *Ubi* promoters, and frequent with *pDD45* or
271 *pRPS5a* driving Cas9 expression (Fig. 3d). We further quantified efficiencies by counting rescued plants
272 across T₂ populations (Fig. 3e). When comparing *Ubi*, *AP1* and *ICU2* promoters, similar genome editing
273 efficiencies of approximately 1% were observed among T₂ plants. Nonetheless, the *Ubi* promoter might
274 perform somewhat better, since all analyzed T₂ populations contained rescued, non-necrotic plants. In clear
275 contrast, rescued plants occurred in all T₂ batches from transformation of *pRPS5a*- and *pDD45*-containing
276 constructs at high frequencies averaging to 33 and 24%, respectively (Fig. 3e). Up to 70% of rescued plants
277 were observed in some T₂ populations, but all still contained necrotic plants, confirming that no homozygous
278 mutants were obtained in the T₁ generation in our experiments. The differences between *RPS5a* and *DD45*
279 promoters observed in our comparison were not statistically significant. Summarizing, our promoter
280 comparison clearly points out superior performance of the *RPS5a* and *DD45* promoters for Arabidopsis
281 genome editing. It should be noted that performance of *pDD45* should be further enhanced by use of the
282 derived “EC1.2-EC1.1 fusion promoter”, which was not tested here (Wang et al., 2015).

283

284

285 High frequency generation of quintuple mutants in T₁ generation with improved Cas9 expression system

286 Having identified regulatory elements suitable for high efficiency Arabidopsis genome editing, the
287 generation of an *lhcb1* mutant line was reattempted. A genome editing construct similar to that shown in
288 Fig. 3a, but containing *pRPS5a*-driven Cas9, a Hygromycin resistance marker cassette (*pnos:hpt-tnos*; instead
289 of *pnos:Bar-tnos*) and the same eight sgRNAs previously used (Fig. 1f) was transformed into a NoMxB3
290 mutant line already defective in *Lhcb4.1*, *Lhcb4.2*, *Lhcb5* and *Lhcb3* genes. T₁ plants were selected by
291 Hygromycin resistance, and further grown in soil. From 30 Hygromycin-resistant plants, 20 showed clearly
292 reduced chlorophyll accumulation in comparison to the parental line, and thus the pale green phenotype
293 expected for reduced *Lhcb1* function (Pietrzykowska et al., 2014). From the 20 plants phenotypically distinct
294 to the NoMxB3 line, 10 had an intermediate phenotype, and the remaining 10 were severely pale (Fig. 4a).
295 To evaluate remaining levels of Lhcb1, leaf tissue samples of three severely pale T₁ plants and the parental
296 NoMxB3 line were used for immunoblot analysis (Fig. 4b). While the control proteins PsaA (PSI core subunit;
297 Mazor et al., 2017) and PsbB/CP47 (PSII core subunit; Wei et al., 2016) were detected to similar levels in all
298 lines, no signal was obtained for Lhcb1 in the genome edited T₁ individuals, suggesting that all five *Lhcb1*
299 genes had been inactivated. The accumulation of light harvesting complex II (LHCII), of which Lhcb1 is a
300 major subunit, was further analyzed by SDS-PAGE and Coomassie staining. Intensity of the major band
301 corresponding to LHCII was strongly reduced in comparison to the parental NoMxB3 line, and we assume
302 that the residual LHCII signal in *lhcb1* genome edited lines originates exclusively from Lhcb2, another LHCII
303 subunit (Liu et al., 2004). PCR-screening with oligonucleotides flanking regions targeted for deletion or
304 mutagenesis indicated complex and diverse rearrangements at the *Lhcb1* loci in putative mutant lines (Fig.
305 4d). In all lines, novel deletion alleles not present in the parental line (ctrl, NoMxB3) were detected. The
306 amplification of multiple PCR products (> 2) from individual lines might result from detection of multiple
307 somatic events (chimeric mutants), or also from low specificity of oligonucleotides due to high homology
308 within *Lhcb1* genes. Analysis of transgene-free T₂ individuals will be required to reveal the precise molecular
309 lesions in putative *lhcb1* lines, and this analysis is yet ongoing. Nonetheless, these results suggest that the
310 improved Cas9 expression system not only enhances overall genome editing frequencies, but even allows
311 the isolation of complex alleles, in this case a quintuple mutant, in a single step in the T₁ generation.

312

313 DISCUSSION

314 Until recently, higher order Arabidopsis mutants could be generated exclusively by crossing of lines
315 harboring the respective lesions. A number of e.g. quintuple, hexuple or even up to decuple mutants were
316 previously reported (e.g. Fujii et al., 2011; Maekawa et al., 2012; Wild et al., 2016), but their isolation is

317 extremely laborious due to segregation of multiple alleles and/or close linkage between loci of interest.
318 Accordingly, it was previously stated that due to “close genetic linkage, loss-of-function (quintuple *Lhcb1* or
319 triple *Lhcb2*) T-DNA KO mutants are almost impossible to generate” (Pietrzykowska et al., 2014). The
320 application of SSNs as reverse genetics tools theoretically alleviated these limitations, but commonly
321 suffered from low efficiency in first reports. Here, by using an optimized Cas9-based genome editing system
322 with high multiplexing capacity, we show that complex alleles such as higher order (quintuple) mutants may
323 be generated with high efficiency even in a single generation (T_1). This demonstrates how SSNs can, through
324 current and future optimization steps, match the increasingly complex demands and requirements of basic
325 research projects in the Arabidopsis model system. The finding that the egg-cell specific promoters (*DD45*
326 and especially the EC1.2-EC1.1 fusion promoter) or the *RPS5a* promoter confer particularly high genome
327 editing efficiencies readily in the T_1 generation (Wang et al., 2015; Tsutsui and Higashiyama, 2017) is by itself
328 not new, but is shown here to withstand direct comparison with other promoter systems using identical
329 vector architectures and sgRNAs/target sites. Vector maps and sequence details for optimized vectors also
330 providing positive/negative selection used here (Fig. 3) are provided in Online Resource 2. Vectors allow
331 simple Golden Gate-based assembly of multiplexing constructs containing up to eight sgRNAs in four days
332 without any PCR steps as previously described (Ordon et al., 2017), and are available upon request.

333 The expression of Cas9 under control of the *DD45* or *RPS5a* promoters improved genome editing efficiencies
334 at the *DM2h* locus approximately 25-fold in comparison to *ubiquitin*, *AP1* and *ICU2* promoters (Fig. 3).
335 Nonetheless, we were successful in isolating a 70 kb deletion allele produced by the previous, non-optimized
336 system containing *ubiquitin* promoter-controlled Cas9 (Fig. 1). This validates the used strategy of PCR-
337 screening large numbers of pooled T_2 individuals and may act as guidance for future isolation of deletion
338 alleles for functional interrogation of gene clusters or non-coding regions. However, this strategy is obviously
339 hampered by lacking controls for functionality of the conducted PCR prior to detection of the desired
340 deletion allele. Interestingly, we estimated the occurrence of the 70 kb deletion allele to approximately 1.6%
341 of T_2 individuals, but detected editing at the *DM2h* locus (in promoter comparison experiments, Fig. 3)
342 among only 1% of T_2 individuals under similar Cas9 expression conditions. Our previous data suggested that
343 point mutations were the most frequent type of Cas9-induced alleles in Arabidopsis, and that the frequency
344 of deletion alleles (between sgRNA target sites in multiplexing applications) was inversely correlated with
345 deletion size, as also reported in at least some studies from animal systems (Canver et al., 2014; Ordon et al.,
346 2017). Taken together, this suggests poor efficiency of the sgRNAs used for *DM2h* editing, which may also
347 explain failure to isolate hetero- or homozygous *dm2h* mutants in the T_1 generation when using *DD45* or
348 *RPS5a* promoters. Indeed, mutations in the T_1 generation were also rare when the *GLABRA2* locus was
349 targeted with *DD45*-driven Cas9 (Mao et al., 2016), supporting that recovery of T_1 -edited plants might
350 strongly depend on sgRNAs and/or target sites. Notably, all of the $\Delta dm2a-g$ deletion alleles detected by PCR

351 screening and further analyzed were heritable, and segregated at Mendelian ratios in respective T₃
352 generations (Fig. 1d), suggesting that detection of somatic genome editing events is not a major issue for
353 isolation of deletions at least under the used conditions.

354 An optimal genome editing system for reverse genetics in Arabidopsis will produce homozygous mutants at
355 near 100% efficiency in the T₁ generation at any given locus. Although the optimization of Cas9 expression
356 conditions tremendously improved efficiencies, further modifications are required to obtain this goal. In
357 respect to Cas9 regulatory sequences, we here focused on previously reported elements, and it is well
358 conceivable that yet uncharacterized promoters and/or transcriptional terminators might further improve
359 genome editing efficiencies. However, also all remaining components may be further optimized, and
360 additional functionalities implemented into T-DNA constructs. To this end, e.g. nuclear import of Cas9 might
361 be enhanced by different or additional nuclear localization signals, or its expression improved by codon
362 optimization or addition of introns. Furthermore, especially sgRNA expression levels appear to have a major
363 influence on a system's performance. To date, sgRNAs were mainly expressed directly from Polymerase III
364 (Pol III)-transcribed U3/U6 promoters. Additionally, sgRNAs were expressed as polycistronic transcripts from
365 Polymerase II (Pol II)-transcribed promoters, and mature sgRNAs are subsequently produced by cleavage
366 through Csy4, self-cleaving ribozymes or the endogeneous tRNA processing system (Gao and Zhao, 2014;
367 Nissim et al., 2014; Xie et al., 2015; Tang et al., 2016). Different Pol III promoters and Pol II-driven ribozyme,
368 tRNA and Csy4 systems were recently systematically compared for genome editing in tomato protoplasts.
369 The Csy4 and tRNA systems improved genome editing efficiencies approximately two-fold in comparison to
370 Pol III-driven sgRNAs (Cermak et al., 2017). However, similar as for the nuclease itself, Pol II promoters
371 providing strong and timely expression in the embryo will most likely be required to improve RGN efficiency
372 by these approaches in Arabidopsis. Recently, also an optimized sgRNA scaffold developed for mammalian
373 cells was reported to enhance editing efficiencies in rice, and in particular the abundance of biallelic and
374 double mutants increased (Dang et al., 2015; Hu et al., 2018). We have now also implemented this improved
375 sgRNA backbone to our system, but are awaiting experimental data to confirm improved efficiency. It should
376 be noted that Cermak et al. (2017) did not observe improved efficiencies when employing a similar
377 optimized sgRNA architecture (Chen et al., 2013). Additional to optimizing components or expression of the
378 RGN system itself, e.g. co-expression of the exonuclease Trex2 was reported to improve genome editing
379 efficiencies ~ two-fold in tomato and barley protoplasts (Cermak et al., 2017). Exonuclease co-expression
380 concomitantly augmented average deletion size, which may facilitate initial mutation detection and simplify
381 design of genetic markers. The described approaches provide ample opportunities to further boost genome
382 editing efficiencies in the Arabidopsis systems towards the development of an optimal reverse genetic tool.
383 Based on our findings that *RPS5a* and egg cell specific promoters confer highest genome editing efficiencies,
384 we propose that one of the well-characterized vector systems incorporating these elements (e.g. Wang et

385 al., 2015; Tsutsui and Higashiyama, 2017; or as described here) should be included for any further
386 benchmarking of Cas9-based RGNs in Arabidopsis.

387

388 AUTHOR CONTRIBUTIONS

389 JS and JO conceived the work, performed experiments and analyzed data. CK performed experiments. MB,
390 LD'O and RB conceived *Lhcb1*-related experiments, and MB performed experiments. JS wrote the manuscript
391 with contributions from all authors.

392

393 FIGURE LEGENDS

394 **Fig. 1:** *Ubiquitin* promoter-driven Cas9 for generation of complex alleles

395 (a) Schematic drawing of the *DM2* cluster from accession Landsberg *erecta* (not drawn to scale). The location
396 of sgRNA target sites and PCR primers for screening (1382/1383) is indicated.

397 (b) PCR-screening of pooled DNAs for occurrence of a $\Delta dm2a-g$ allele. Each pool contained 7-11 T₂
398 individuals from transformation of the $\Delta dm2a-g$ genome editing construct. A size of ~ 500 bp is expected
399 upon deletion of *DM2a-g*. PCR products were resolved on a 1% agarose gel and DNA visualized with
400 ethidium bromide.

401 (c) Deconvolution of pools to identify single plants carrying the $\Delta dm2a-g$ deletion allele. DNA was extracted
402 from single plants of pools #8 and #89 from (b), and PCR-screened for a $\Delta dm2a-g$ deletion as before. The
403 parental line (ctrl) and a previously PCR-positive pool DNA were used as controls.

404 (d) Inheritability and segregation of the $\Delta dm2a-g$ deletion allele in the T₃ generation. DNA was extracted
405 from single T₃ plants derived from plant #36 in (c), and was used for genotyping: Presence of $\Delta dm2a-g$,
406 presence of *DM2c*, and presence of Cas9. Results shown are representative for several independent T₃
407 populations analyzed in parallel. Two individuals homozygous for $\Delta dm2a-g$ (absence of *DM2c*) are boxed.

408 (e) Molecular lesion in a $\Delta dm2a-g$ deletion line. The amplicon from (d) representing the $\Delta dm2a-g$ deletion
409 was sequenced directly. The sgRNA target sites are indicated.

410 (f) Genetic organization of the two *Lhcb1* linkage groups on chromosome 1 and chromosome 2 of the
411 Arabidopsis genome (drawn to scale). 1-8 indicate the positioning of sgRNA target sites.

412 **Fig. 2:** Effect of transcription terminators on Cas9 activity in transient reporter assays

413 (a) Architecture of minimalistic nuclease constructs used for systematic comparison of 3'UTR sequences and
414 transcriptional terminators for Cas9 expression.

415 (b) Evaluation of genome editing efficiency of nuclease constructs differing only in Cas9 3'UTR/terminator
416 sequences. A *GUS*-based nuclease activity reporter and different nuclease constructs were transiently co-
417 transformed into *N. benth.* tissues by Agrobacterium infiltration, and GUS activity was determined 3 dpi. Background
418 activity of the reporter alone was arbitrarily set to 1, and GUS activities normalized. A nuclease construct
419 with t35S-terminated Cas9 was included as control (nuclease). Error bars represent standard deviations from
420 four replicates. The experiment was repeated four times with similar results. The following 3'UTR/terminator
421 sequences were used: 35S - 35S terminator from cauliflower mosaic virus; *Atug7* - *Atug7* terminator from
422 *Agrobacterium tumefaciens* (*A. tumefaciens*); *nos* - *nos* terminator from *A. tumefaciens*; *act2* - *Actin2*
423 terminator from *Arabidopsis thaliana*; *mas* - *mas* terminator from *A. tumefaciens*; *ATPase* - *ATPase*
424 terminator from *Solanum lycopersicum* (*S. lycopersicum*); *rbcS C3* - from *S. lycopersicum*; *H4* - *Histone H4*
425 from *Solanum tuberosum* (all Engler et al., 2014, and references therein); *rbcS E9* - from *Pisum sativum*
426 (Wang et al., 2015).

427

428 **Fig. 3:** Systematic comparison of promoters for driving Cas9 expression in *Arabidopsis thaliana*

429 (a) Schematic drawing of constructs used for Arabidopsis transformation. Both sgRNAs are driven by
430 identical fragments of the pU6-26 promoter. Constructs differ only in Cas9 promoter/5'UTR sequences.

431 (b) Functionality of the BASTA resistance marker.

432 (c) Functionality of the FAST marker in T₁ and T₂ generations.

433 (d) Phenotypic survey of genome editing efficiencies with different promoters driving Cas9 expression.

434 Representative pictures of T₂ pools and control plants (*Ler*, *Ler old3-1*) grown at 22°C are shown.

435 (e) Quantitative assessment of genome editing efficiencies. Necrotic/rescued plants from (d) were counted.

436

437 **Fig. 4:** Generation of *Lhcb1* mutant plants in a single generation

438 (a) Phenotype of putative *Lhcb1* mutant plants. The NoMxB3 parental line is shown as control, in comparison
439 to one of the severely pale T₁ lines recovered from Hygromycin selection and editing of *Lhcb1* genes.

440 (b) Immunoblot analysis of Lhcb1 protein accumulation. Protein extracts from the parental NoMxB3 line and
441 three independent T₁ plants putatively deficient in *Lhcb1* genes were used for immunodetection of Lhcb1.

442 PsaA and PsbB/CP47 were detected as control proteins and loading control.

443 (c) Tris-Tricine SDS-PAGE and Coomassie staining of total protein as in (b). The major signal corresponding to
444 LHCB1 is marked, and strongly reduced in genome-edited T₁ individuals due to loss of Lhcb1.
445 (d) PCR interrogation at *Lhcb1* loci in T₁ genome-edited lines. DNA was extracted from T₁ lines and the
446 parental NoMxB3 line (ctrl), and used for PCR with primers flanking outermost sgRNA target sites (Fig. 1f) in
447 *Lhcb1* genes on chromosome 1 (upper panel, PCR *Lhcb1.1/.2/.3*) and chromosome 2 (lower panel, PCR
448 *Lhcb1.4/.5*).

449

450 **Online Resource 1:** Architecture and functional verification of an adaptable, *GUS*-based nuclease activity
451 reporter

452 (a) T-DNA region of the adaptable reporter plasmid, and cloning of user-defined target sequences. The
453 “empty” plasmid contains a 35S-driven *GUS*, with a *BsmBI*-excisable *ccdB* cassette inserted between the
454 initiating ATG and the *GUS* coding sequence. In a *BsmBI* Golden Gate reaction, the *ccdB* cassette is
455 exchanged for a user-defined target sequence introduced as hybridized oligonucleotides. A configuration in
456 which the reporter detects a -1 nt repair event (or e.g. -4 or +2 nt events) is shown as example. The reporter
457 may be adapted to detect different events by varying the length of the introduced target site. It should be
458 noted that the introduced target site may not, after repair, contain an in-frame STOP codon.

459 (b) Functional verification of the *GUS*-based reporter. Two different target sites were introduced into the
460 adaptable plasmid to obtain Reporters 1/2, reporters were co-expressed with respective nucleases in *N.*
461 *benth.*, and GUS activity visualized by X-Gluc 3 dpi. Nuclease/reporter combination 2 consistently showed
462 stronger GUS activity.

463

464 **Online Resource 2:** Sequence details on nuclease and reporter constructs used in this study (annotated
465 GenBank files)

466

467

468

469 REFERENCES

- 470 **Alcazar, R., Garcia, A.V., Parker, J.E., and Reymond, M.** (2009). Incremental steps toward incompatibility
471 revealed by Arabidopsis epistatic interactions modulating salicylic acid pathway activation. PNAS
472 **106**, 334-339.
- 473 **Alcazar, R., Garcia, A.V., Kronholm, I., de Meaux, J., Koornneef, M., Parker, J.E., and Reymond, M.** (2010).
474 Natural variation at *Strubbelig Receptor Kinase 3* drives immune-triggered incompatibilities between
475 *Arabidopsis thaliana* accessions. Nat Genet **42**, 1135-1139.
- 476 **Alcazar, R., von Reth, M., Bautor, J., Chae, E., Weigel, D., Koornneef, M., and Parker, J.E.** (2014). Analysis of
477 a plant complex resistance gene locus underlying immune-related hybrid incompatibility and its
478 occurrence in nature. PLoS Genet **10**, e1004848.
- 479 **Belhaj, K., Chaparro-Garcia, A., Kamoun, S., and Nekrasov, V.** (2013). Plant genome editing made easy:
480 targeted mutagenesis in model and crop plants using the CRISPR/Cas system. Plant Methods **9**, 39.
- 481 **Botella, M.A., Parker, J.E., Frost, L.N., Bittner-Eddy, P.D., Beynon, J.L., Daniels, M.J., Holub, E.B., and Jones,**
482 **J.D.** (1998). Three genes of the Arabidopsis *RPP1* complex resistance locus recognize distinct
483 *Peronospora parasitica* avirulence determinants. Plant Cell **10**, 1847-1860.
- 484 **Canver, M.C., Bauer, D.E., Dass, A., Yien, Y.Y., Chung, J., Masuda, T., Maeda, T., Paw, B.H., and Orkin, S.H.**
485 (2014). Characterization of genomic deletion efficiency mediated by clustered regularly interspaced
486 palindromic repeats (CRISPR)/Cas9 nuclease system in mammalian cells. Journal of Biological
487 Chemistry **289**, 21312-21324.
- 488 **Cesar, S.A., Rajan, V., Prykhozhij, S.V., Berman, J.N., and Ignacimuthu, S.** (2016). Insert, remove or replace:
489 A highly advanced genome editing system using CRISPR/Cas9. Biochimica et Biophysica Acta **1863**,
490 2333-2344.
- 491 **Cermak, T., Curtin, S.J., Gil-Humanes, J., Cegan, R., Kono, T.J.Y., Konecna, E., Belanto, J.J., Starker, C.G.,**
492 **Mathre, J.W., Greenstein, R.L., and Voytas, D.F.** (2017). A multi-purpose toolkit to enable advanced
493 genome engineering in plants. Plant Cell **29**, 1196–1217.
- 494 **Chae, E., Bomblies, K., Kim, S.T., Karelina, D., Zaidem, M., Ossowski, S., Martin-Pizarro, C., Laitinen, R.A.,**
495 **Rowan, B.A., Tenenboim, H., Lechner, S., Demar, M., Habring-Muller, A., Lanz, C., Ratsch, G., and**
496 **Weigel, D.** (2014). Species-wide genetic incompatibility analysis identifies immune genes as hot
497 spots of deleterious epistasis. Cell **159**, 1341-1351.
- 498 **Chavez, A., Tuttle, M., Pruitt, B.W., Ewen-Campen, B., Chari, R., Ter-Ovanesyan, D., Haque, S.J., Cecchi,**
499 **R.J., Kowal, E.J., Buchthal, J., Housden, B.E., Perrimon, N., Collins, J.J., and Church, G.** (2016).
500 Comparison of Cas9 activators in multiple species. Nat Methods **13**, 563-567.

501 **Chen, B., Hu, J., Almeida, R., Liu, H., Balakrishnan, S., Covill-Cooke, C., Lim, W.A., and Huang, B.** (2016).
502 Expanding the CRISPR imaging toolset with *Staphylococcus aureus* Cas9 for simultaneous imaging of
503 multiple genomic loci. *Nucleic Acids Res* **44**, e75.

504 **Chen, B., Gilbert, L.A., Cimini, B.A., Schnitzbauer, J., Zhang, W., Li, G.W., Park, J., Blackburn, E.H.,**
505 **Weissman, J.S., Qi, L.S., and Huang, B.** (2013). Dynamic imaging of genomic loci in living human cells
506 by an optimized CRISPR/Cas system. *Cell* **155**, 1479-1491.

507 **Dall'Osto, L., Cazzaniga, S., Bressan, M., Palecek, D., Zidek, K., Niyogi, K.K., Fleming, G.R., Zigmantas, D.,**
508 **and Bassi, R.** (2017). Two mechanisms for dissipation of excess light in monomeric and trimeric light-
509 harvesting complexes. *Nat Plants* **3**, 17033.

510 **Dang, Y., Jia, G., Choi, J., Ma, H., Anaya, E., Ye, C., Shankar, P., and Wu, H.** (2015). Optimizing sgRNA
511 structure to improve CRISPR-Cas9 knockout efficiency. *Genome Biology* **16**, 280.

512 **Desfeux, C., Clough, S.J., and Bent, A.F.** (2000). Female reproductive tissues are the primary target of
513 *Agrobacterium*-mediated transformation by the *Arabidopsis* floral-dip method. *Plant Phys* **123**, 895-
514 904.

515 **Doench, J.G., Hartenian, E., Graham, D.B., Tothova, Z., Hegde, M., Smith, I., Sullender, M., Ebert, B.L.,**
516 **Xavier, R.J., and Root, D.E.** (2014). Rational design of highly active sgRNAs for CRISPR-Cas9-mediated
517 gene inactivation. *Nature Biotech* **32**, 1262-1267.

518 **Doench, J.G., Fusi, N., Sullender, M., Hegde, M., Vaimberg, E.W., Donovan, K.F., Smith, I., Tothova, Z.,**
519 **Wilen, C., Orchard, R., Virgin, H.W., Listgarten, J., and Root, D.E.** (2016). Optimized sgRNA design to
520 maximize activity and minimize off-target effects of CRISPR-Cas9. *Nature Biotech* **34**, 184-191.

521 **Dominguez, A.A., Lim, W.A., and Qi, L.S.** (2016). Beyond editing: repurposing CRISPR-Cas9 for precision
522 genome regulation and interrogation. *Nature Reviews* **17**, 5-15.

523 **Eid, A., Ali, Z., and Mahfouz, M.M.** (2016). High efficiency of targeted mutagenesis in *Arabidopsis* via meiotic
524 promoter-driven expression of Cas9 endonuclease. *Plant Cell Reports* **35**, 1555-1558.

525 **Engler, C., Kandzia, R., and Marillonnet, S.** (2008). A one pot, one step, precision cloning method with high
526 throughput capability. *PLoS ONE* **3**, e3647.

527 **Engler, C., Youles, M., Gruetzner, R., Ehnert, T.M., Werner, S., Jones, J.D., Patron, N.J., and Marillonnet, S.**
528 (2014). A Golden Gate Modular Cloning Toolbox for Plants. *ACS Synthetic Biology*.

529 **Fausser, F., Schiml, S., and Puchta, H.** (2014). Both CRISPR/Cas-based nucleases and nickases can be used
530 efficiently for genome engineering in *Arabidopsis thaliana*. *Plant Journal* **79**, 348-359.

531 **Feng, Z., Zhang, B., Ding, W., Liu, X., Yang, D.L., Wei, P., Cao, F., Zhu, S., Zhang, F., Mao, Y., and Zhu, J.K.**
532 (2013). Efficient genome editing in plants using a CRISPR/Cas system. *Cell Res* **23**, 1229-1232.

533 **Fujii, H., Verslues, P.E., and Zhu, J.K.** (2011). *Arabidopsis* decuple mutant reveals the importance of SnRK2
534 kinases in osmotic stress responses *in vivo*. *PNAS* **108**, 1717-1722.

535 **Galka, P., Santabarbara, S., Thi, T.H.K., Degand, H., Morsomme, P., Jennings, R.C., Boekema, E.J., and**
536 **Caffarri, S.** (2012). Functional Analyses of the Plant Photosystem I-Light-Harvesting Complex II
537 Supercomplex Reveal That Light-Harvesting Complex II Loosely Bound to Photosystem II Is a Very
538 Efficient Antenna for Photosystem I in State II. *Plant Cell* **24**, 2963-2978.

539 **Gao, Y., and Zhao, Y.** (2014). Self-processing of ribozyme-flanked RNAs into guide RNAs *in vitro* and *in vivo*
540 for CRISPR-mediated genome editing. *Journal of Integr Plant Biol* **56**, 343-349.

541 **Gao, Y., Zhang, Y., Zhang, D., Dai, X., Estelle, M., and Zhao, Y.** (2015). Auxin binding protein 1 (ABP1) is not
542 required for either auxin signaling or Arabidopsis development. *PNAS* **112**, 2275-2280.

543 **Hu, X., Meng, X., Liu, Q., Li, J., and Wang, K.** (2018). Increasing the efficiency of CRISPR-Cas9-VQR precise
544 genome editing in rice. *Plant Biotechnol Journal* **16**, 292-297.

545 **Huang, S., Weigel, D., Beachy, R.N., and Li, J.** (2016). A proposed regulatory framework for genome-edited
546 crops. *Nat Genet* **48**, 109-111.

547 **Hyun, Y., Kim, J., Cho, S.W., Choi, Y., Kim, J.S., and Coupland, G.** (2015). Site-directed mutagenesis in
548 *Arabidopsis thaliana* using dividing tissue-targeted RGEN of the CRISPR/Cas system to generate
549 heritable null alleles. *Planta* **241**, 271-284.

550 **Jinek, M., Chylinski, K., Fonfara, I., Hauer, M., Doudna, J.A., and Charpentier, E.** (2012). A programmable
551 dual-RNA-guided DNA endonuclease in adaptive bacterial immunity. *Science* **337**, 816-821.

552 **Komor, A.C., Kim, Y.B., Packer, M.S., Zuris, J.A., and Liu, D.R.** (2016). Programmable editing of a target base
553 in genomic DNA without double-stranded DNA cleavage. *Nature* **533**, 420-424.

554 **Labun, K., Montague, T.G., Gagnon, J.A., Thyme, S.B., and Valen, E.** (2016). CHOPCHOP v2: a web tool for
555 the next generation of CRISPR genome engineering. *Nucleic Acids Res* **44**, W272-276.

556 **Liang, Z., Chen, K., Li, T., Zhang, Y., Wang, Y., Zhao, Q., Liu, J., Zhang, H., Liu, C., Ran, Y., and Gao, C.** (2017).
557 Efficient DNA-free genome editing of bread wheat using CRISPR/Cas9 ribonucleoprotein complexes.
558 *Nat Commun* **8**, 14261.

559 **Liu, Z., Yan, H., Wang, K., Kuang, T., Zhang, J., Gui, L., An, X., and Chang, W.** (2004). Crystal structure of
560 spinach major light-harvesting complex at 2.72 Å resolution. *Nature* **428**, 287-292.

561 **Logemann, E., Birkenbihl, R.P., Ulker, B., and Somssich, I.E.** (2006). An improved method for preparing
562 *Agrobacterium* cells that simplifies the Arabidopsis transformation protocol. *Plant Methods* **2**, 16.

563 **Maekawa, T., Kracher, B., Vernaldi, S., Ver Loren van Themaat, E., and Schulze-Lefert, P.** (2012).
564 Conservation of NLR-triggered immunity across plant lineages. *PNAS* **109**, 20119-20123.

565 **Malzahn, A., Lowder, L., and Qi, Y.** (2017). Plant genome editing with TALEN and CRISPR. *Cell Biosci* **7**, 21.

566 **Mao, Y., Zhang, H., Xu, N., Zhang, B., Gou, F., and Zhu, J.K.** (2013). Application of the CRISPR-Cas system for
567 efficient genome engineering in plants. *Mol Plant* **6**, 2008-2011.

568 **Mao, Y., Zhang, Z., Feng, Z., Wei, P., Zhang, H., Botella, J.R., and Zhu, J.K.** (2016). Development of germ-line-
569 specific CRISPR-Cas9 systems to improve the production of heritable gene modifications in
570 Arabidopsis. *Plant Biotechnol Journal* **14**, 519-532.

571 **Mazor, Y., Borovikova, A., Caspy, I., and Nelson, N.** (2017). Structure of the plant photosystem I
572 supercomplex at 2.6 Å resolution. *Nat Plants* **3**, 17014.

573 **Mikami, M., Toki, S., and Endo, M.** (2015). Comparison of CRISPR/Cas9 expression constructs for efficient
574 targeted mutagenesis in rice. *Plant Molecular Biology* **88**, 561-572.

575 **Nissim, L., Perli, S.D., Fridkin, A., Perez-Pinera, P., and Lu, T.K.** (2014). Multiplexed and programmable
576 regulation of gene networks with an integrated RNA and CRISPR/Cas toolkit in human cells.
577 *Molecular Cell* **54**, 698-710.

578 **Ordon, J., Gantner, J., Kemna, J., Schwalgun, L., Reschke, M., Streubel, J., Boch, J., and Stüttmann, J.**
579 (2017). Generation of chromosomal deletions in dicotyledonous plants employing a user-friendly
580 genome editing toolkit. *Plant Journal* **89**, 155-168.

581 **Osakabe, Y., Watanabe, T., Sugano, S.S., Ueta, R., Ishihara, R., Shinozaki, K., and Osakabe, K.** (2016).
582 Optimization of CRISPR/Cas9 genome editing to modify abiotic stress responses in plants. *Scientific*
583 *Reports* **6**, 26685.

584 **Peterson, B.A., Haak, D.C., Nishimura, M.T., Teixeira, P.J., James, S.R., Dangl, J.L., and Nimchuk, Z.L.** (2016).
585 Genome-Wide Assessment of Efficiency and Specificity in CRISPR/Cas9 Mediated Multiple Site
586 Targeting in Arabidopsis. *PLoS ONE* **11**, e0162169.

587 **Pietrzykowska, M., Suorsa, M., Semchonok, D.A., Tikkanen, M., Boekema, E.J., Aro, E.M., and Jansson, S.**
588 (2014). The light-harvesting chlorophyll a/b binding proteins Lhcb1 and Lhcb2 play complementary
589 roles during state transitions in Arabidopsis. *Plant Cell* **26**, 3646-3660.

590 **Ran, F.A., Hsu, P.D., Lin, C.Y., Gootenberg, J.S., Konermann, S., Trevino, A.E., Scott, D.A., Inoue, A.,**
591 **Matoba, S., Zhang, Y., and Zhang, F.** (2013). Double nicking by RNA-guided CRISPR Cas9 for
592 enhanced genome editing specificity. *Cell* **154**, 1380-1389.

593 **Ren, B., Yan, F., Kuang, Y., Li, N., Zhang, D., Zhou, X., Lin, H., and Zhou, H.** (2018). Improved base editor for
594 efficiently inducing genetic variations in rice with CRISPR/Cas9-guided hyperactive *hAID* mutant. *Mol*
595 *Plant*.

596 **Schagger, H., and von Jagow, G.** (1987). Tricine-sodium dodecyl sulfate-polyacrylamide gel electrophoresis
597 for the separation of proteins in the range from 1 to 100 kDa. *Anal Biochem* **166**, 368-379.

598 **Shi, J., Gao, H., Wang, H., Lafitte, H.R., Archibald, R.L., Yang, M., Hakimi, S.M., Mo, H., and Habben, J.E.**
599 (2017). *ARGOS8* variants generated by CRISPR-Cas9 improve maize grain yield under field drought
600 stress conditions. *Plant Biotechnol Journal* **15**, 207-216.

601 **Shimada, T.L., Shimada, T., and Hara-Nishimura, I.** (2010). A rapid and non-destructive screenable marker,
602 FAST, for identifying transformed seeds of *Arabidopsis thaliana*. *Plant Journal* **61**, 519-528.

603 **Stuttman, J., Peine, N., Garcia, A.V., Wagner, C., Choudhury, S.R., Wang, Y., James, G.V., Griebel, T.,**
604 **Alcazar, R., Tsuda, K., Schneeberger, K., and Parker, J.E.** (2016). *Arabidopsis thaliana DM2h (R8)*
605 within the Landsberg *RPP1-like* Resistance Locus Underlies Three Different Cases of EDS1-
606 Conditioned Autoimmunity. *PLoS Genet* **12**, e1005990.

607 **Su, X., Ma, J., Wei, X., Cao, P., Zhu, D., Chang, W., Liu, Z., Zhang, X., and Li, M.** (2017). Structure and
608 assembly mechanism of plant C2S2M2-type PSII-LHCII supercomplex. *Science* **357**, 815-820.

609 **Tahir, J., Watanabe, M., Jing, H.C., Hunter, D.A., Tohge, T., Nunes-Nesi, A., Brotman, Y., Fernie, A.R.,**
610 **Hoefgen, R., and Dijkwel, P.P.** (2013). Activation of R-mediated innate immunity and disease
611 susceptibility is affected by mutations in a cytosolic O-acetylserine (thiol) lyase in *Arabidopsis*. *Plant*
612 *Journal* **73**, 118-130.

613 **Tang, X., Zheng, X., Qi, Y., Zhang, D., Cheng, Y., Tang, A., Voytas, D.F., and Zhang, Y.** (2016). A Single
614 Transcript CRISPR-Cas9 System for Efficient Genome Editing in Plants. *Mol Plant* **9**, 1088-1091.

615 **Tang, X., Lowder, L.G., Zhang, T., Malzahn, A.A., Zheng, X., Voytas, D.F., Zhong, Z., Chen, Y., Ren, Q., Li, Q.,**
616 **Kirkland, E.R., Zhang, Y., and Qi, Y.** (2017). A CRISPR-Cpf1 system for efficient genome editing and
617 transcriptional repression in plants. *Nat Plants* **3**, 17018.

618 **Tsutsui, H., and Higashiyama, T.** (2017). pKAMA-ITACHI Vectors for Highly Efficient CRISPR/Cas9-Mediated
619 Gene Knockout in *Arabidopsis thaliana*. *Plant Cell Physiol* **58**, 46-56.

620 **Wang, Z.P., Xing, H.L., Dong, L., Zhang, H.Y., Han, C.Y., Wang, X.C., and Chen, Q.J.** (2015). Egg cell-specific
621 promoter-controlled CRISPR/Cas9 efficiently generates homozygous mutants for multiple target
622 genes in *Arabidopsis* in a single generation. *Genome Biology* **16**, 144.

623 **Weber, E., Engler, C., Gruetzner, R., Werner, S., and Marillonnet, S.** (2011). A modular cloning system for
624 standardized assembly of multigene constructs. *PLoS ONE* **6**, e16765.

625 **Wei, X., Su, X., Cao, P., Liu, X., Chang, W., Li, M., Zhang, X., and Liu, Z.** (2016). Structure of spinach
626 photosystem II-LHCII supercomplex at 3.2 Å resolution. *Nature* **534**, 69-74.

627 **Wild, M., Daviere, J.M., Regnault, T., Sakvarelidze-Achard, L., Carrera, E., Lopez Diaz, I., Cayrel, A.,**
628 **Dubeaux, G., Vert, G., and Achard, P.** (2016). Tissue-Specific Regulation of Gibberellin Signaling Fine-
629 Tunes *Arabidopsis* Iron-Deficiency Responses. *Developmental Cell* **37**, 190-200.

630 **Wolt, J.D., Wang, K., and Yang, B.** (2016). The Regulatory Status of Genome-edited Crops. *Plant Biotechnol*
631 *Journal* **14**, 510-518.

632 **Woo, J.W., Kim, J., Kwon, S.I., Corvalan, C., Cho, S.W., Kim, H., Kim, S.G., Kim, S.T., Choe, S., and Kim, J.S.**
633 (2015). DNA-free genome editing in plants with preassembled CRISPR-Cas9 ribonucleoproteins.
634 *Nature Biotech* **33**, 1162-1164.

635 **Xiao, A., Cheng, Z., Kong, L., Zhu, Z., Lin, S., Gao, G., and Zhang, B.** (2014). CasOT: a genome-wide
636 Cas9/gRNA off-target searching tool. *Bioinformatics*.

637 **Xie, K., Minkenberg, B., and Yang, Y.** (2015). Boosting CRISPR/Cas9 multiplex editing capability with the
638 endogenous tRNA-processing system. *PNAS* **112**, 3570-3575.

639 **Yan, L., Wei, S., Wu, Y., Hu, R., Li, H., Yang, W., and Xie, Q.** (2015). High-Efficiency Genome Editing in
640 Arabidopsis Using YAO Promoter-Driven CRISPR/Cas9 System. *Mol Plant* **8**, 1820-1823.

641 **Ye, G.N., Stone, D., Pang, S.Z., Creely, W., Gonzalez, K., and Hinchee, M.** (1999). Arabidopsis ovule is the
642 target for *Agrobacterium in planta* vacuum infiltration transformation. *Plant Journal* **19**, 249-257.

643 **Zhang, Y., Liang, Z., Zong, Y., Wang, Y., Liu, J., Chen, K., Qiu, J.L., and Gao, C.** (2016). Efficient and transgene-
644 free genome editing in wheat through transient expression of CRISPR/Cas9 DNA or RNA. *Nat*
645 *Commun* **7**, 12617.

Figure 1 Ordon et al.

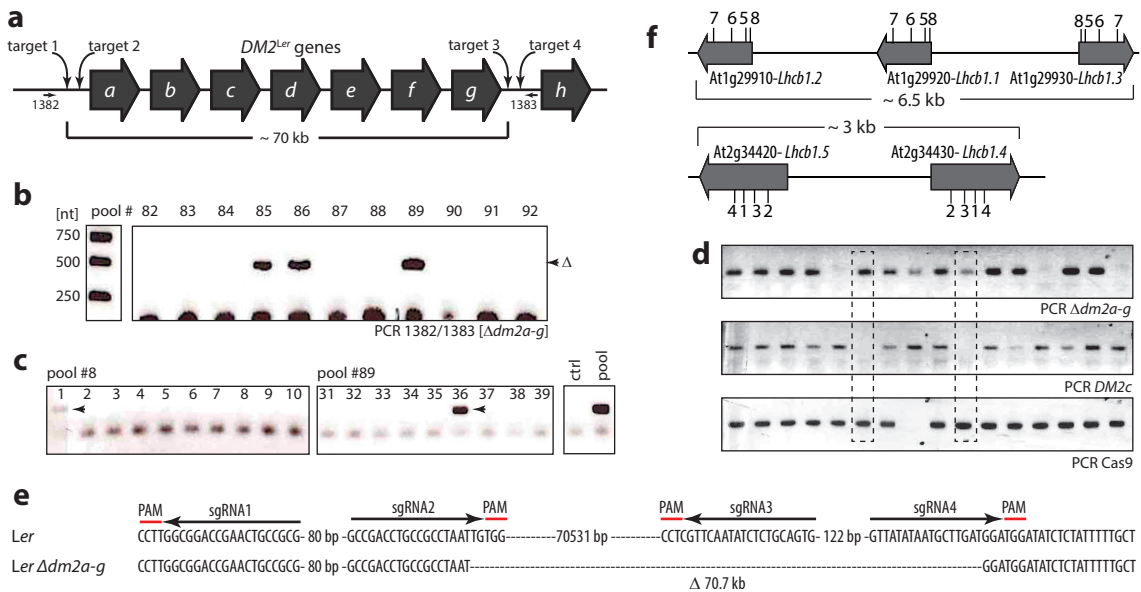


Fig. 1: Ubiquitin promoter-driven Cas9 for generation of complex alleles

(a) Schematic drawing of the *DM2* cluster from accession Landsberg *erecta* (not drawn to scale). The location of sgRNA target sites and PCR primers for screening (1382/1383) is indicated.

(b) PCR-screening of pooled DNAs for occurrence of a $\Delta dm2a-g$ allele. Each pool contained 7-11 T_2 individuals from transformation of the $\Delta dm2a-g$ genome editing construct. A size of ~ 500 bp is expected upon deletion of *DM2a-g*. PCR products were resolved on a 1% agarose gel and DNA visualized with ethidium bromide.

(c) Deconvolution of pools to identify single plants carrying the $\Delta dm2a-g$ deletion allele. DNA was extracted from single plants of pools #8 and #89 from (b), and PCR-screened for a $\Delta dm2a-g$ deletion as before. The parental line (ctrl) and a previously PCR-positive pool DNA were used as controls.

(d) Inheritability and segregation of the $\Delta dm2a-g$ deletion allele in the T_3 generation. DNA was extracted from single T_3 plants derived from plant #36 in (c), and was used for genotyping: Presence of $\Delta dm2a-g$, presence of *DM2c*, and presence of Cas9. Results shown are representative for several independent T_3 populations analyzed in parallel. Two individuals homozygous for $\Delta dm2a-g$ (absence of *DM2c*) are boxed.

(e) Molecular lesion in a $\Delta dm2a-g$ deletion line. The amplicon from (d) representing the $\Delta dm2a-g$ deletion was sequenced directly. The sgRNA target sites are indicated.

(f) Genetic organization of the two *Lhcb1* linkage groups on chromosome 1 and chromosome 2 of the Arabidopsis genome (drawn to scale). 1-8 indicate the positioning of sgRNA target sites.

Figure 2 Ordon et al.

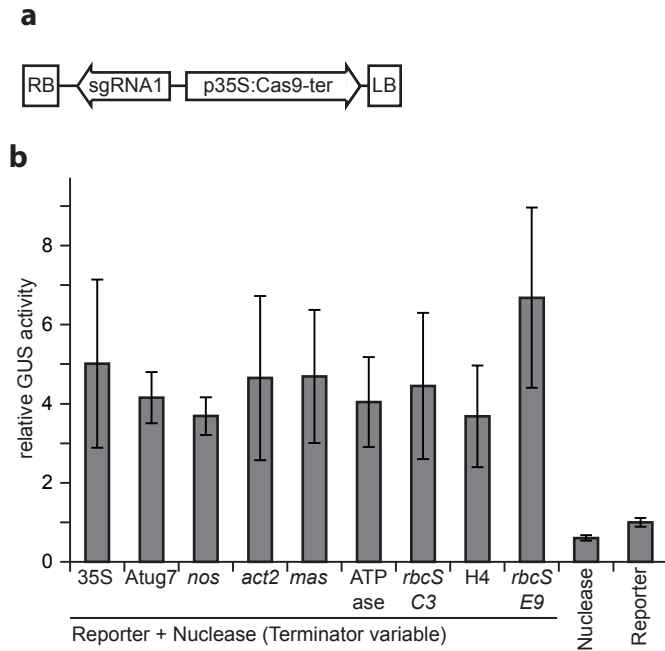


Fig. 2: Effect of transcription terminators on Cas9 activity in transient reporter assays

(a) Architecture of minimalistic nuclease constructs used for systematic comparison of 3'UTR sequences and transcriptional terminators for Cas9 expression.

(b) Evaluation of genome editing efficiency of nuclease constructs differing only in Cas9 3'UTR/terminator sequences. A GUS-based nuclease activity reporter and different nuclease constructs were transiently co-transformed into *N. benthamiana* tissues by Agroinfiltration, and GUS activity was determined 3 dpi. Background activity of the reporter alone was arbitrarily set to 1, and GUS activities normalized. A nuclease construct with t35S-terminated Cas9 was included as control (nuclease). Error bars represent standard deviations from four replicates. The experiment was repeated four times with similar results. The following 3'UTR/terminator sequences were used: 35S - 35S terminator from cauliflower mosaic virus; Atug7 - Atug7 terminator from *Agrobacterium tumefaciens* (*A. tumefaciens*); nos - nos terminator from *A. tumefaciens*; act2 - Actin2 terminator from *Arabidopsis thaliana*; mas - mas terminator from *A. tumefaciens*; ATPase - ATPase terminator from *Solanum lycopersicum* (*S. lycopersicum*); rbcS C3 - from *S. lycopersicum*; H4 - Histone H4 from *Solanum tuberosum* (all Engler et al., 2014, and references therein); rbcS E9 - from *Pisum sativum* (Wang et al., 2015).

Figure 3 Ordon et al.

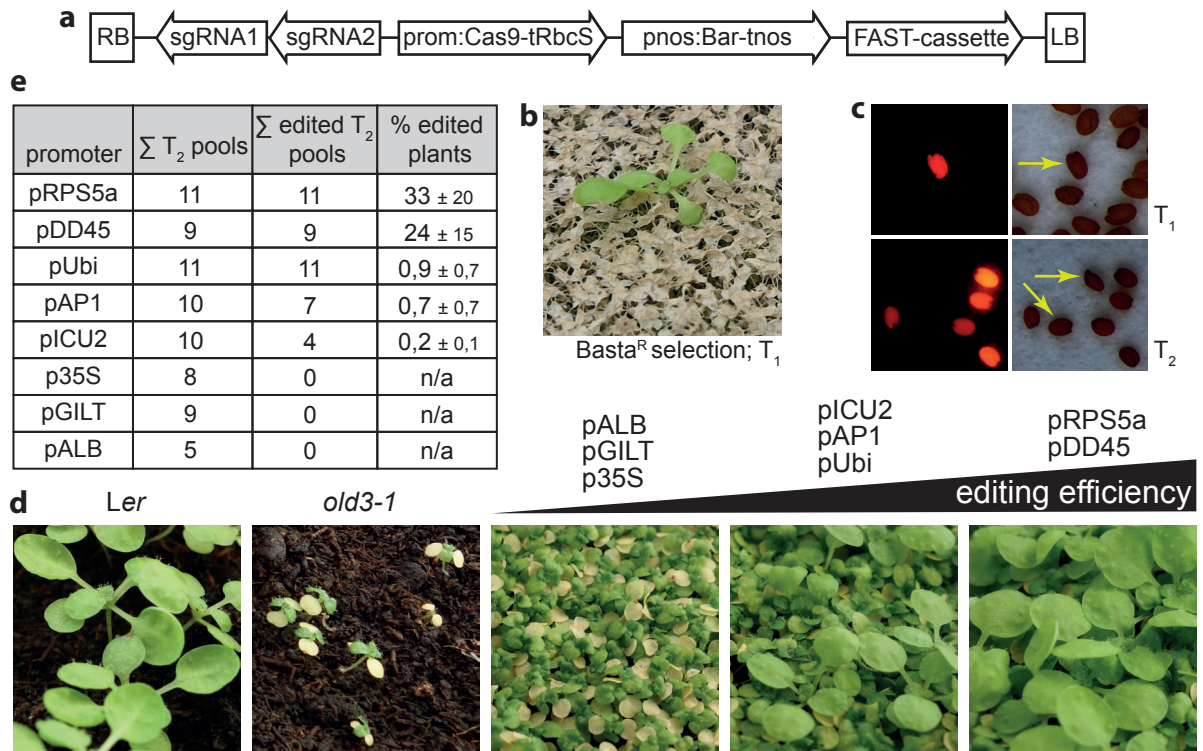


Fig. 3: Systematic comparison of promoters for driving Cas9 expression in *Arabidopsis thaliana*
 (a) Schematic drawing of constructs used for Arabidopsis transformation. Both sgRNAs are driven by identical fragments of the pU6-26 promoter. Constructs differ only in Cas9 promoter/5'UTR sequences.
 (b) Functionality of the BASTA resistance marker.
 (c) Functionality of the FAST marker in T₁ and T₂ generations.
 (d) Phenotypic survey of genome editing efficiencies with different promoters driving Cas9 expression. Representative pictures of T₂ pools and control plants (*Ler*, *Ler old3-1*) grown at 22°C are shown.
 (e) Quantitative assessment of genome editing efficiencies. Necrotic/rescued plants from (d) were counted.

Figure 4 Ordon et al.

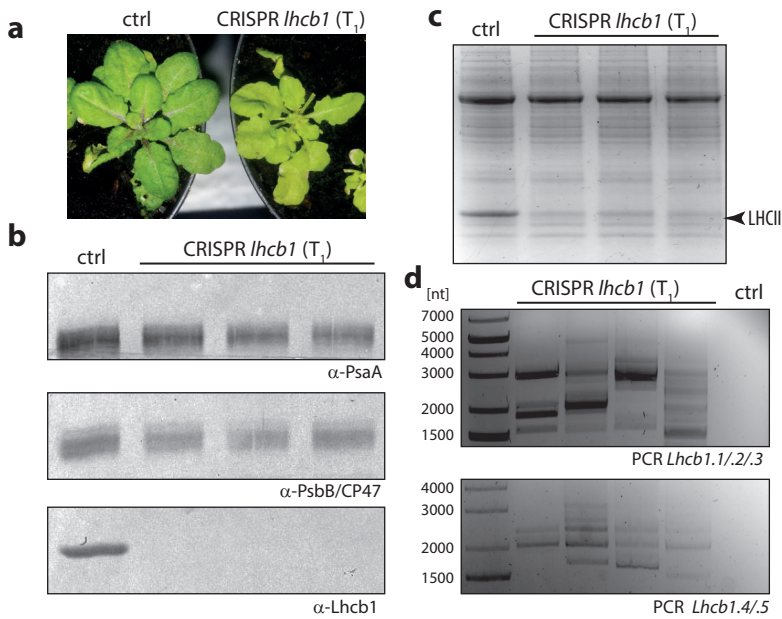


Fig. 4: Generation of *Lhcb1* mutant plants in a single generation

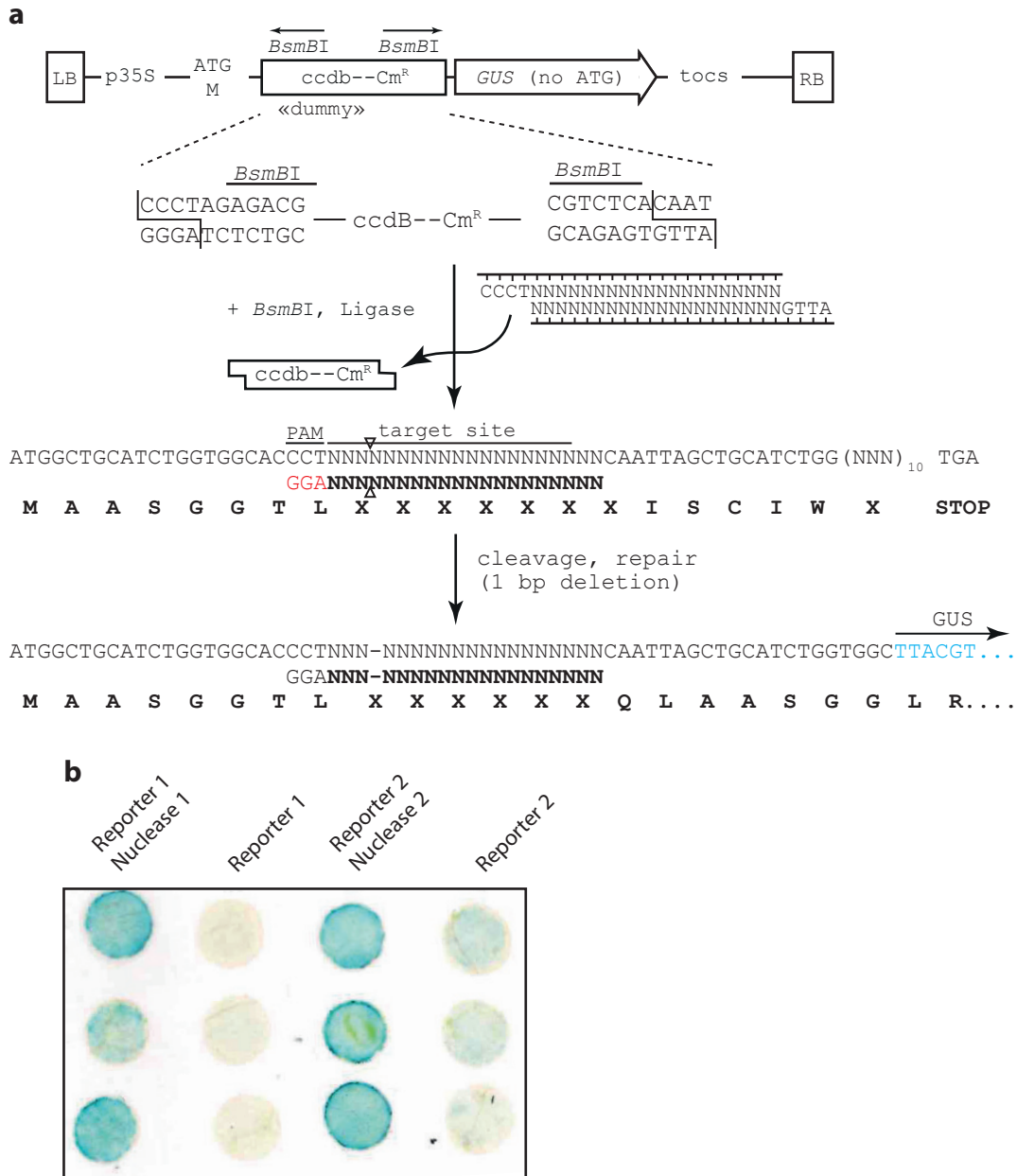
(a) Phenotype of putative *Lhcb1* mutant plants. The NoMxB3 parental line is shown as control, in comparison to one of the severely pale T₁ lines recovered from Hygromycin selection and editing of *Lhcb1* genes.

(b) Immunoblot analysis of *Lhcb1* protein accumulation. Protein extracts from the parental NoMxB3 line and three independent T₁ plants putatively deficient in *Lhcb1* genes were used for immunodetection of Lhcb1. PsaA and PsbB/CP47 were detected as control proteins and loading control.

(c) Tris-Tricine SDS-PAGE and Coomassie staining of total protein as in (b). The major signal corresponding to LHCII is marked, and strongly reduced in genome-edited T₁ individuals due to loss of Lhcb1.

(d) PCR interrogation at *Lhcb1* loci in T₁ genome-edited lines. DNA was extracted from T₁ lines and the parental NoMxB3 line (ctrl), and used for PCR with primers flanking outermost sgRNA target sites (Fig. 1f) in *Lhcb1* genes on chromosome 1 (upper panel, PCR *Lhcb1.1/.2/.3*) and chromosome 2 (lower panel, PCR *Lhcb1.4/.5*).

Supplemental Figure 1 Ordon et al.



Supplemental Figure S1: Architecture and functional verification of an adaptable, *GUS*-based nuclease activity reporter

(a) T-DNA region of the adaptable reporter plasmid, and cloning of user-defined target sequences. The “empty” plasmid contains a 35S-driven *GUS*, with a *BsmBI*-excisable *ccdB* cassette inserted between the initiating ATG and the *GUS* coding sequence. In a *BsmBI* Golden Gate reaction, the *ccdB* cassette is exchanged for a user-defined target sequence introduced as hybridized oligonucleotides. A configuration in which the reporter detects a -1 nt repair event (or e.g. -4 or +2 nt events) is shown as example. The reporter may be adapted to detect different events by varying the length of the introduced target site. It should be noted that the introduced target site may not, after repair, contain an in-frame STOP codon.

(b) Functional verification of the *GUS*-based reporter. Two different target sites were introduced into the adaptable plasmid to obtain Reporters 1/2, reporters were co-expressed with respective nucleases in *N. benth.*, and GUS activity visualized by X-Gluc 3 dpi. Nuclease/reporter combination 2 consistently showed stronger GUS activity.